# Horizontal humidity gradient from a single scanning microwave radiometer

J. H. Schween, S. Crewell, U. Löhnert

*University of Cologne, Zülpicher Str. 49a, 50674 Köln, Germany, jschween@uni-koeln.de*

## 1. INTRODUCTION

Water vapour, the most important greenhouse gas, also plays a crucial role within the hydrological cycle. Its spatial distribution is determined by advection, the processes of evaporation at the surface and cloud-forming/dissipation. Their correct description still provides large challenges for current weather forecast and climate models. In particular, water vapour variations in the boundary layer influence the development of convective precipitation and are therefore important for quantitative precipitation forecasting. Several methods for observing water vapour with high spatial and temporal resolution have been suggested. Microwave radiometry (MWR) is one of the most promising methods as it is a robust, highly automated technique for nearly all weather conditions. The major limitation of MWR is due to the limited vertical resolution providing only 2-3 independent pieces of information (Löhnert et al., 2009). However, Kneifel et al. (2009) could demonstrate that the water vapour column can be observed with high accuracy to provide spatial and temporal variability. In this paper we present a new approach to derive horizontal gradients of water vapour from a single MWR in volume scanning mode. Such data are potentially useful to identify convergence zones, front development and evaluate atmospheric models.

## 2. METHOD

Integrated water vapour (IWV) sometimes referred to as precipitable water or water vapour column abbreviated here as $W$ is the integral over water vapour density along a line of sight. We are interested in how an inhomogeneous water vapour field appears in measured $W$-values. As a first order linear approach we assume for the water vapour density in the boundary layer ($z<h$) a constant gradient $A_1$ in $x$-direction. For the vertical we assume a constant water vapour density $A_0$ in the boundary layer and an exponential decay with scaling length $L$ in the free troposphere above. This water vapour distribution is integrated along the line of sight yielding equation (1) for the airmass corrected water vapour column:

$$W(\alpha,\theta) = W_1 \tan(\theta)\cos(\alpha+\varphi) + W_0 \quad (1)$$

with azimuth angle $\alpha$, zenith angle $\theta$ and direction of the gradient $\phi$. Despite the correction for the relative airmass the amplitude of the cosine still depends on the zenith angle via $\tan\theta$. This is due to the fact that with increasing zenith angle the horizontal gradient has a stronger influence than close to the zenith. The offset $W_0$ is the water vapour column in the vertical and related to profile parameters via

$$W_0 = A_0 \cdot (h + L) \quad (2)$$

with $A_0$ the average humidity of the boundary layer (g m$^{-3}$), where $A_0 \cdot h$ is the water vapour column of the boundary layer and $A_0 \cdot L$ the water vapour column of the free troposphere. The factor $q = h/L$ gives the partitioning of water vapour between both parts of the atmosphere. The amplitude $W_1$ of the cosine wave in equation (1) depends on the horizontal gradient $A_1$:

$$W_1 = A_1 \cdot \left(\tfrac{1}{2}h^2 + h \cdot L + L^2\right) \quad (3)$$

Therefore the amplitude depends not only on the humidity gradient $A_1$ but also on the parameters $h$ and $L$ describing the form of the water vapour profile. Parameters $W_0$ and $W_1$ and $\phi$ can be determined by means of a least square fit to data from a scanning microwave radiometer. Parameters $A_o$, $h$ and $L$ must be derived from water vapour density profiles.

## 3. INSTRUMENTATION

Integrated water vapour column is observed by a scanning Humidity and Temperature Profiler (HATPRO; Rose et al., 2005) installed at the research center Jülich at 50° 54' 30.77" N, 6° 24' 48.73" E, 93 m ASL. IWV is derived via statistical algorithms (Löhnert and Crewell, 2003) from brightness temperature measurements in three channels along the 22.235 GHz water vapour emission line. HATPRO scans the whole upper hemisphere every 18min in steps of 10°(azimuth) and 9.6°(zenith). At each position the measurement takes one second, the whole volume scan takes about 8.25 minutes and consists of 360 data points. The antenna first points to the South with low elevation (zenith angle 86.4°) and moves to zenith direction. Then the azimuth angle is adjusted one step (10°) to the East and the elevation mirror moves to the horizon again. This pattern is continued until the full hemisphere has been observed. Because the antenna beam width (full width at half maximum, FWHM) is about 3.5°, the largest zenith angle of 86.4°, i.e. 3.6° elevation, should be just above the horizon. Nevertheless, trees and other obstacles close to the horizon lead to contamination of the data that we do not use. As an example we here present data from September 9, 2009 where also five radiosondes (Graw DFM06) were launched from a site about 6 km south of the HATPRO instrument between 8 and 17 UTC.

## 3. WEATHER SITUATION

September 9, 2009 was characterized by an occluding front slowly approaching the site from the northwest. At 00 UTC the front was located about 200 km away from the site stretching from the southern coast of Great Britain to the northeast. During 9 September the system approached the site, however, only passing it in the early morning of the following day. Therefore September 9 was cloud free until around 12 UTC when thin cirrus and cirrocumulus clouds started to indicate the approach of the front. Around 15 UTC

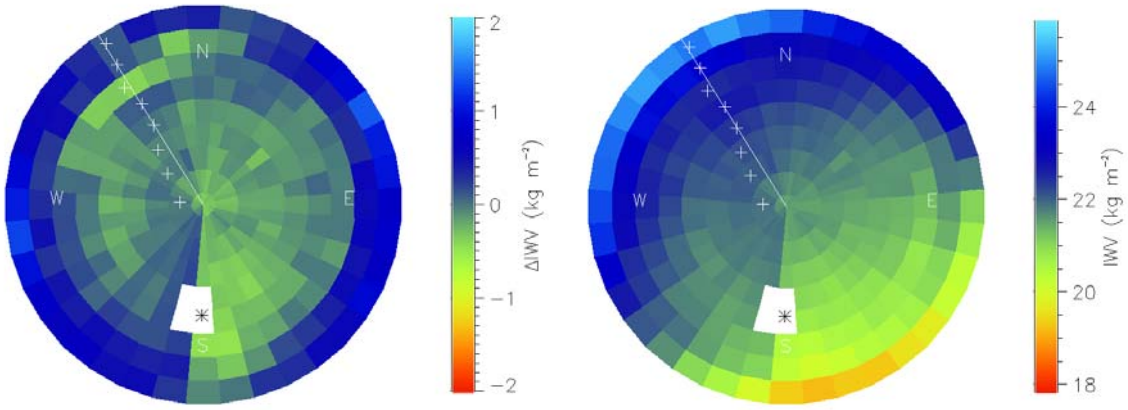


*Figure 1. Hemispheric distribution of water vapour column derived from HATPRO measurements between 11:30 and 11:38 UTC (left) and residual after the fitted linear gradient has been subtracted (right). The zenith angle of the outermost ring is $\theta = 76.8°$. The asterisk gives the position of the sun, plus signs indicate the gradient direction inferred from fits to individual zenith angles and the radial line indicates the direction of the gradient derived from the full volume data.*

altocumulus clouds began to cover the sky. Temperatures reached 27°C and remained above 25°C until 15:30 UTC. Wind speed at 2 m increased during the day from nearly zero to 4 $ms^{-1}$ in the afternoon. In the lower boundary layer (below 400 m) measurements by a nearby SODAR show weak wind speeds below 2 $ms^{-1}$ with no clear direction until 12 UTC when winds turned from northwest to north and increased to 5 $ms^{-1}$ at 16 UTC. Data from the HATPRO showed a continuous increase of the zenith water vapour column from 11 kg $m^{-2}$ (00 UTC) to 31 kg $m^{-2}$ (16 UTC) indicating the advection of moist air ahead of the front.

## 4. WATER VAPOUR GRADIENT

In total 79 hemispheric scans were performed on September 9. Nearly all scans show a similar structure with highest *W* values in the northwest, indicating that the approaching front was associated with a more humid air mass. As an example the scan at 11:30 UTC (Fig. 1) shows values between 19.2 $kgm^{-2}$ and 25.1 $kgm^{-2}$ at the largest zenith angle $\theta = 76.8°$. At $\theta = 57.6°$ the values range between 20.5 $kgm^{-2}$ and 22.8 $kgm^{-2}$. This amplitude can nearly completely be described by the linear gradient model. The second dominant structure visible in the residuum is a pronounced jump in IWV between two successive azimuth angles in the south with lower values to the east and higher values to west. This is connected to a temporal change of the field during the scan, which starts with southern directions, runs counterclockwise towards the east and returns after 8.25 minutes back to south from the west. Because only the first four azimuth angles are affected this indicates a significant increase in water vapour during the first minute of the scan.

In order to estimate the horizontal water vapour gradient the parameters $A_o$, *h* and *L* of equations (2) and (3) need to be known. On September 9, 2009 the five radiosondes and also ceilometer measurements indicate a relatively constant boundary layer height with $h = 1100$ m. Therefore, for the highest zenith angle of $\theta = 76.8°$, i.e. lowest elevation, the radiometer receives information from the boundary layer over a distance of 4.7 km. Water vapour density within the boundary layer $A_0$ is calculated as the average below *h* for each of the five radiosoundings of the day. The scaling length *L* for the exponential decay in the free troposphere is determined from the zenith water vapour column of the radiometer measurements $W_0$ following (2) as $L = W_0 / A_0 - h$. The use of the zenith data is preferred against the radiosonde data since the later drifted with the wind in south-eastern direction and is therefore influenced by the horizontal water vapour gradient. Analysis of the profile data reveals that at 8 UTC 49% of the water vapour is located in the Boundary Layer. At 16 UTC this value has reduced to 40% while water vapour density in the Boundary layer has increased by 48%. To compensate for this vertical water vapour column of the free troposphere must have increased by 43%.

For each scan the model from equation (1) was fitted to the full volume data. For the example scan in Fig. 1 this yields cosine wave amplitude $W_1$ of about 0.5 $kgm^{-2}$, horizontal water vapour density gradient $A_1$ of about 0.1 $gm^{-3}km^{-1}$ and direction $\phi$ of about 320° (NW). The residual IWV (Fig. 1) shows a highly variable structure, which could arise from irregularly distributed convective elements. The lowest elevations exhibit a positive bias that might arise from beam width effects in combination with atmospheric refraction. A negative bias can be seen for the first azimuth angles of the scan as already mentioned above. We can conclude that the linear model explains most of the IWV variations ($R^2 = 0.8$). In addition to the full volume fit, the model was also fitted to each zenith angle, i.e. to each ring in Fig. 1, individually. The resulting gradient directions (Fig. 1) do not differ by more than 5° (for zenith angles larger than 20°) confirming the assumption that a linear horizontal gradient describes the situation fairly well.

During the course of the day a continuous rise in IWV is observed (Fig. 2). The gradient $A_1$ is always positive and rises up to its day maximum of 0.14 $gm^{-3}km^{-1}$ at

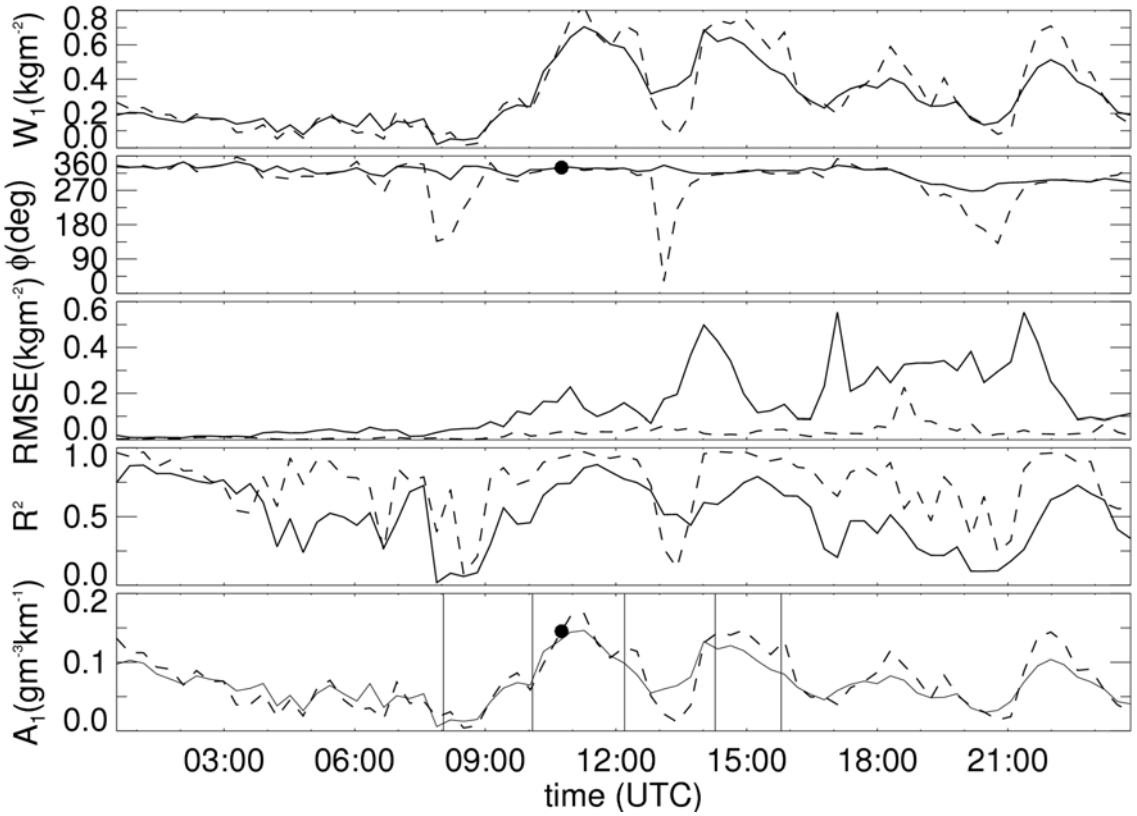


***Figure 2**. Derived parameters from the HATPRO scan data for the full scan (solid line) and for $\theta = 57.6°$ (dashed line). From top to bottom: Amplitude $W_1$ of the cosine wave (1), direction $\phi$ of the gradient, root mean square error of the model (RMSE), coefficient of determination ($R^2$) and calculated gradient $A_1$. Vertical lines in the lowermost plot indicate radiosonde launch times. The symbols at 10:48 UTC mark the direction and amplitude of the gradient derived from MERIS data.*

11 UTC, which corresponds to the strongest increase of water vapour in the free troposphere. The second maximum around 14 UTC coincides with the strongest increase of $A_0$ in the boundary layer. The amplitude $W_1$ for the whole scan and for the single-$\theta$ fit at $\theta = 57.6°$ agree most of the time very well indicating that the whole field on that day is sufficiently described by the linear gradient model. However, there are deviations between the whole scan and the single-$\theta$ fit. They are connected to low $R^2$ values for either of the models i.e. when the variance in the water vapour field cannot be described with the model. RMSE of the fit to the whole field is always larger than the single-$\theta$ fit. This is mainly due to the larger amplitude observed at the lowest elevation, which cannot be described well by the model. The larger values in the second part of the day might be explained by enhanced turbulent activity and cloud occurrence in the area. Gradient direction $\phi$ is nearly constant at northwest until 18 UTC when it turns slightly to west. There is good agreement between the whole-scan-fit and the single-$\theta$-fit except for the times with low $R^2$.

In order to evaluate the quality of the derived gradients with an independent method, data from Medium Resolution Imaging Spectrometer Instrument (MERIS) onboard of ENVISAT are suitable due to their fine spatial resolution of up to 300 m. Water vapour columns from the overpass at 10:48 UTC were used to derive the gradient from differences over 8 km distance. Division by $h+L$ gives the gradient $A_1$ of the water vapour concentration. The agreement both for direction and amplitude is nearly perfect with deviations of less than 5 %.

## 5. SUMMARY AND CONCLUSION

We presented a method to continuously derive water vapour gradients from a single scanning microwave radiometer. The method requires the knowledge of parameters characterizing the water vapour profile which can be gained from the MWR itself and information on boundary layer height from a close by ceilometer. An example day revealed a rather persistent north-westerly gradient with an amplitude varying between 0 and 0.14 $gm^{-3}km^{-1}$. This amplitude exhibited distinct maxima that occurred at different times for the boundary layer and free troposphere contribution.

The consistency of results derived by fitting the full volume and single zenith angles indicates that it might be advantageous to reduce the scan pattern to one or two zenith angles. This would reduce the scanning time and therefore avoid jumps between the start and stop elevation angle. In addition, a higher temporal resolution would be possible. The assumptions about the water vapour profile, i.e. constant density in boundary layer and exponential decay in the free troposphere, helped to achieve an explained variance of about 0.7 most of the time. This could not be achieved by simpler profile assumptions. In the future

we want to investigate more than one year of volume scan data from the Jülich site taken within the German priority program TR32 ”Patterns in Soil-Vegetation-Atmosphere Systems: Monitoring, Modelling and Data Assimilation”. In particular we want to identify dominant patterns over long time scales, assess the goodness of the linear model and investigate whether the residuum can be linked to convective activity.

## References


Kneifel, S., S. Crewell, U. Löhnert and J. Schween, 2009: Investigating water vapor variability by ground-based microwave radiometry: Evaluation using airborne observations. *IEEE Geoscience and Remote Sensing Letters*, **6(1)**, 157-161, DOI.10.1109 / LGRS.2008.2007659.

Löhnert, U., and S. Crewell, 2003: Accuracy of cloud liquid water path from ground-based microwave radiometry. Part I: Dependency on cloud model statistics and precipitation. *Radio Sci*. **38**, 8041, doi:10.1029/2002RS002654.

Löhnert, U., D. Turner, S. Crewell, 2009: Ground-based temperature and humidity profiling using spectral infrared and microwave observations: Part 1. Simulated retrieval performance in clear sky conditions. *J. Appl. Meteorol. Clim*. **48(5)**, 1017–1032, DOI: 10.1175/2008JAMC2060.1

Rose, T., S. Crewell, U. Löhnert, and C. Simmer, 2005: A network suitable microwave radiometer for operational monitoring of the cloudy atmosphere. *Atmos. Res*. **75**, 183-200.